Tellus (2002), 54B, 163–185
Printed in UK. All rights reserved

TELLUS
ISSN 0280–6509

Highlights of the tropospheric lidar studies at IFU within the TOR project

By W. CARNUTH, U. KEMPFER and T. TRICKL, *Fraunhofer-Institut für atmosphärische Umweltforschung (IFU), Kreuzeckbahnstrasse 19, D-82467 Garmisch-Partenkirchen, Germany*

(Manuscript received 9 September 2000; in final form 15 November 2001)

ABSTRACT

A summary of the ozone soundings with the tropospheric ozone lidar at IFU in the years 1991 and 1993 is given. The results cover vertical distributions obtained under a variety of meteorological conditions in different seasons such as during high pressure, before and after frontal passages and during stratospheric air intrusions. The lidar time series, carried out between typically 0.25 and 10 km and at intervals of about 1 h, are an excellent tool for transport studies. Quite frequently contributions of different processes may be observed even simultaneously which may yield insight on the troposphere as a whole. Although the time series were limited to single days during that phase information on a number of relevant transport processes could be extracted. In particular, the uplifting in the Alpine thermal wind system was investigated. The air in the valley is vented to heights in part even beyond 4 km a.s.l. during fair-weather summer days. The high efficiency of the underlying mechanism suggests a major contribution of the orographically induced transport in the Alps to the pollution export from the Central European boundary layer. A spectacular case of trans-Alpine ozone transport was examined which resulted in an ozone increase by about 40% after sunset. This case may, again, reflect the role of the Alps in the redistribution of air pollution in a larger area. In addition, episodes of long-range ozone and aerosol transport have been studied. In this paper, we present the example of intense Föhn with advection of dust-loaded air from the Sahara desert and beyond containing just 35 ppb of O_3. A rather complex layering may be observed after cold-front passages associated with subsequent anticyclonic advection. The analysis of a two-day vertical-sounding series reveals that the air in different height ranges originated in the troposphere or stratosphere above rather different source regions, even in the lowermost 4 km above the United States. More recent studies have confirmed the reproducibility of the general layer pattern under such conditions. The in part considerable difference in ozone concentration makes the definition of a free-tropospheric background ozone level a difficult task.

1. Introduction

In the past two decades there have been intensified efforts to investigate the mechanisms which govern the formation and distribution of tropospheric ozone. Many of the processes involved are now increasingly well understood. Models have started to yield a better approach to the experimental findings. However, there are still considerable gaps and discrepancies which necessitate major research efforts in the near future.

One of these tasks must be more concentrated studies of the processes influencing the vertical distribution of ozone and its precursors. For many years, information on tropospheric ozone was derived mostly from the data acquired at ground-based monitoring stations which form a rather dense network. However, unless such stations are in part located on mountains the measurements

* Corresponding author.
e-mail: trickl@ifu.fhg.de

performed there are representative of the true ozone load of the planetary boundary layer (PBL) only in the presence of strong vertical mixing due to the influence of deposition or chemical decomposition. Information on the free troposphere requires measurements above the height of typical summit stations which can only be contributed by vertical sounding or aircraft flights. Compared with the density of ground-based in-situ monitors, that of vertical sounding stations has been low. All over Europe just a few stations launch balloons with ozone sondes on a regular basis. These launches take place at intervals of 2–3 days, and thus do not suffice to resolve diurnal cycles or short-term variations, but may provide a valuable basis for climatological studies. The alternative approach, aircraft-based measurements, offers the advantage of yielding both the vertical and the horizontal distribution of important constituents. Due to the high flight costs such investigations can be run only in concentrated campaigns.

The most promising method for high-density ground-based vertical sounding has been lidar. Lidar is already a mature technique for stratospheric ozone monitoring, but tropospheric systems had, until the end of the 1980s (and in part until now), not reached the full level of reliability needed. For ground-based tropospheric systems substantially more demanding technical tasks are imposed by the greatly enhanced dynamical range of the backscatter signal, caused by the necessity of a low start altitude, preferably below 200 m. Additional problems are the presence of aerosols, clouds as well as anthropogenically emitted trace gases such as SO_2, NO_2 and hydrocarbons, which all absorb light in the same ultraviolet (UV) spectral range as O_3, and the solar signal background. A European effort to develop lidar systems for routine measurements of tropospheric ozone has been coordinated within the TESLAS (Tropospheric Environmental Studies by Laser Sounding) subproject of the EUROTRAC project (TESLAS, 1997) and has yielded several state-of-the-art ground-based instruments which gradually have entered scientific operation. Nevertheless, ground-based systems with sufficient vertical range and accuracy are rare, even on a world-wide scale (e.g. Ansmann et al., 1997; Proffitt and Langford, 1997; Singh et al., 1998). A range from next to the ground to at least 4 km is also desirable for smaller systems, but is rarely met.

At IFU (Fraunhofer-Institut für Atmosphärische Umweltforschung), a tropospheric lidar with a particularly wide vertical range of typically 0.25–10 km was completed within TESLAS as early as 1990. A detailed description of this system was given by Kempfer et al. (1994). It could be demonstrated that, at least in the lower troposphere, the accuracy level of conventional in-situ monitors may almost be reached. In this paper, we mostly discuss a first annual series carried out in 1991 comprising as many as 580 individual measurements. These measurements were carried out within the TOR (Tropospheric Ozone Research) subproject of EUROTRAC (TOR, 1997, 1997a).

Within TOR, vertical sounding was limited to a few stations, only three of them equipped with ozone lidars which were run in rather different operating ranges (e.g. Ancellet et al., 1991, 1994; Ancellet and Beekmann, 1997; Bösenberg et al., 1997; this work). This situation is to some extent due the late beginning of the system development in TESLAS. Despite the limited lidar activities the results obtained demonstrate the importance of dense vertical-sounding time series in characterizing the atmospheric processes influencing the variation of ozone at different altitudes. Our efforts in the early 1990s are the basis of the work continued in more recent years, and already match major topics of current research programmes.

As will be evident from the examples shown in this paper, the most valuable contribution of lidar sounding are transport studies. The lidar time series yield information on both vertical and horizontal transport, and thus contribute to principal topics of the TOR project. Vertical exchange was focussed on in two special task groups of TOR (Beck et al., 1997; Beekmann et al., 1997a, 1997b). In particular, an extensive analysis of stratosphere–troposphere exchange (STE) in tropopause folds was carried out, based on the analysis of sonde data and model results. Descending stratospheric air layers may be traced in detail by lidar measurements (e.g. Browell et al., 1987; Ancellet et al., 1991, 1994; Langford et al., 1996). However, although we observed several stratospheric air intrusions we do not include a section on STE in this paper. A topic of growing importance is long-range transport of ozone. Medium- and long-range transport creates trace-gas and aerosol signatures throughout the troposphere and influences

the ozone concentration in a complex manner. This touches the TOR key question about the magnitude of the background ozone concentration over Europe.

By starting the lidar measurements an old tradition of vertical ozone sounding at IFU was resumed. Between 1978 and 1985, 458 ozonesonde ascents took place (Reiter et al., 1985). In order to obtain more detailed information an ECC ozone monitor was mounted on the cable car from Eibsee to Zugspitze (1000 m to 2950 m a.s.l.) (Reiter et al., 1987; Reiter, 1990). A total of 1990 such measurements were carried out between 1980 and 1982. Results on the variation of the ozone concentration in the PBL and on subsidence of stratospheric air down to altitudes below that of the Zugspitze summit were obtained. In addition to these measurements a continuous record of ozone and other trace gases has been accumulated at the mountain-top stations Wank (1780 m a.s.l.) and Zugspitze (2940 m a.s.l.) since 1978 (Sladkovic et al., 1994, 1997). Trends have been analysed and show an increase of the ozone mixing ratio measured at both stations of 1–2 ppb a^{-1} in the period 1978–1983 and substantially less afterwards (Sladkovic et al., 1994; Scheel et al., 1999).

The paper is organized as follows: Section 2 gives a brief technical description of the lidar system. In Section 3 selected examples of ozone distributions are shown and analysed which illustrate the temporal evolution of the O_3 concentration in the PBL and the FT for a variety of typical conditions. In Section 4 a more general discussion is given. Section 5 summarizes the conclusions obtained after the first few years of lidar operation and outlines some recent developments.

2. Description of the lidar system

2.1. Technical description

A full system description was published by Kempfer et al. (1994). Here we give the most important features of the design and performance of our differential-absorption lidar (DIAL).

The transmitter section consists of a narrow-band krypton fluoride excimer laser, a Raman cell filled with hydrogen and a 5:1 beam expander. Due to the linear polarization of the KrF laser a high Raman conversion efficiency for the first three Stokes orders is achieved even at low pressures. For the DIAL measurements we use the first- and second-Stokes output of the Raman shifter at 277.2 and 313.2 nm. The best simultaneous conversion efficiency for these two wavelengths is 30%, which corresponds to a pulse energy of 60 mJ under optimum conditions. The beam expander reduces the beam divergence, which is enhanced by the stimulated Raman shifting, to less than 0.4 mrad (full angle).

Due to a near-field signal maximum at 100 m and the rapid signal decay towards higher altitudes the dynamic range of the backscatter signal covers more than eight decades. In order to avoid detection nonlinearities we divide this range into near and far field by using two separate receivers, Newtonian telescopes with 13 and 50 cm diameter, respectively. The large telescope is displaced from the laser beam axis by 1.6 m. Thus, the intense near-field light, which would cause an over-exposure of the photomultiplier tubes, may be blocked by an aperture. The large mirror collects an enhanced amount of light and is sufficiently sensitive for measurements in the upper troposphere. The signals from the large telescope are used for the ozone evaluation in the range above 1.5 km.

In addition to the geometrical range division the gain of all the four detectors is switched from low to high as soon as the signal drops to a level at which it is affected by noise and poorely smoothed single-bit steps of the 8-bit analogue-to-digital converters. Due to a negligible solar background single-photon counting is applied in the far-field 277-nm channel because this technique is significantly less susceptible to electromagnetic interference, gain instabilities and signal-induced errors (Section 2.2).

The technical concept chosen has made possible an operating range which, in principle, covers the entire troposphere between 0.2 and 12 km above ground. A range up to 12 km is, however, achieved only for moderate tropospheric ozone densities, which are most frequently found in winter. In summer, the elevated ozone concentrations lead to additional absorption at 277 nm and a upper boundary sometimes not exceeding 8 km.

The lidar is located in the top floor of IFU, at an altitude of about 740 m a.s.l. (47°28′37″N, 11°03′52″E). The IFU summit stations Zugspitze (2940 m a.s.l.) and Wank (1780 m a.s.l.) are located at distances less than 10 km from the institute. Garmisch-Partenkirchen and the institute are

located in the Loisach valley about 20 km before it exits from the Alps, 80 km roughly south of Munich.

2.2. Data evaluation and error considerations

In the majority of cases the data evaluation yields a reliability of the ozone number density within $7 \times 10^{-16}\,\mathrm{m}^{-3}$ (i.e. 3.1 ppb next to the ground and 6.9 ppb at 8 km above ground). Due to the large number of data channels and their segmentation the evaluation algorithm is not straightforward. The ozone number density is obtained by applying a polynomial-fitting approach to the logarithm of the ratio of the range-corrected backscatter profiles for the 'on' and 'off' wavelengths, followed by derivative formation (Kempfer et al., 1994). Since the signal-to-noise ratio decreases with growing vertical distance, the range resolution is dynamically reduced to compensate for this effect. For the interval sequence chosen a rather constant density error is achieved, with the exception of the uppermost 1–2 km of the useful range. The effective vertical intervals (Kempfer et al., 1994) applied for the data evaluation typically vary from about 0.03 km in regions with good signal quality to 0.8 km in the upper troposphere. In some cases with lower signal-to-noise ratio additional smoothing with a numerical low-pass filter (over range bins of 0.1–0.2 km) is applied.

The ozone number density obtained from the backscatter profiles is converted into mixing ratios by using a model air number density. After observing inconsistencies of the LOWTRAN 7 temperature and pressure models an alternative model was derived from a simultaneous least-squares fit to temperature and pressure data of the Munich radio sonde for the days of interest in 1991:

$$P\ (\mathrm{mbar}) = 1013.287 \exp(-0.114\,599h - 0.001\,750h^2) \quad (1)$$

and

$$T\ (\mathrm{K}) = 292.08 - 6.7581h, \quad (2)$$

h being the absolute height in km.

$n = P/(kT)$ from this model reproduces the number densities calculated from the radiosonde data below the tropopause within typically $\pm 2\%$, which implies a partial cancellation of the seasonal variation of P and T by the division. The deviation of the number densities calculated with eqs. (1) and (2) from the 1977 US Standard Atmosphere is $\pm 1.3\%$ up to 9 km, $+1.9\%$ at 11 km and $+5.4\%$ at 12 km a.s.l.

The errors of the backscatter data are rather small, which is crucial for the evaluation of accurate ozone values because it is based on derivative formation. The excellent performance of our system for 313 nm could be verified by inspecting Rayleigh-corrected profiles [see Fig. 11 of Kempfer et al. (1994)]. However, minor deviations existed for 277 nm which are visible in part because of the faster signal decay in the 277-nm channels to a level at which perturbations may be observed. Due to our system design the deviations were to a major extent not due to the signal-induced distortions traditionally described in the literature (e.g. Iikura et al., 1987; Lee at al., 1990; McDermid et al., 1990; Bristow et al., 1995). They were mainly caused by signal ringing in the near-field channels and fluorescence of the 277-nm interference filters, and were most pronounced in the earliest data due to admitting rather high signal levels and fast rise times. The necessary small local corrections (of the order of 10–15% in ozone) are quality-controlled by intercomparison of overlapping parts of the different 277-nm data channels, in final reference to the photon-counting data. Based on this strategy the diurnal series of the examples shown in this paper and several additional days have been completely re-evaluated. The improvements in detection electronics in a subsequent period have led to an elimination of the time-consuming corrections, resulting in the applicability of an automatic evaluation procedure, at least in cases of moderate aerosol concentrations.

The aerosol interference was treated by conventional methods based on the evaluation of the 313-nm backscatter profile (Kempfer et al., 1994). Due to the prevailing high visibility at our site the reliability of this correction is satisfactory, as confirmed by routine intercomparison with our mountain-top in-situ stations. The results in layers with haze or rapidly changing cloud coverage may be unacceptable and have been eliminated.

3. Results

The short time for a single measurement of just a few minutes makes possible high-density time

series of vertical ozone profiles. The diurnal series have been taken at intervals of 1–2 h, which are sufficient in most cases to monitor the changes in the troposphere. In 1991, single-day series were carried out on a few days per month selected from a more demonstrational than climatological point of view. A reasonable coverage of a major part of the entire year is obtained (January to September), but measurements were not carried out during the full length of extended episodes. A total of 580 measurements were made on altogether 80 d, which may be some of the most intensive series of vertical soundings ever performed in a single year to that date.

The examples shown in the following sections cover a variety of ozone distributions for different seasons and meteorological conditions and are representative of many topics of ongoing tropospheric ozone research. The analysis is based on available meteorological and summit station data. Wherever needed, tabulated radio-sonde data have been inspected for comparison. Recently, isentropic trajectories for the Zugspitze summit station were calculated by NOAA (National Oceanic and Atmospheric Administration) CMDL for all days back to 1990 (0000 and 1200 UTC) which allow some conclusions to be made for air masses arriving at 3000 m (Harris and Kahl, 1990; Harris et al., 1992).

Despite the promising results, the measurements (and also further system development) had to be stopped for some time after 1991. In summer 1993 the measurements were resumed for a few months at a low rate. Data were taken on a few days mainly in collaboration with the OCTA (Oxidizing Capacity of the Tropospheric Atmosphere, European Union, 1993–1994) project or during a UVB sensor intercomparison campaign.

3.1. Boundary layer

The structure of the PBL may conveniently be traced by the vertical distribution of the aerosol backscatter coefficients β_P (P denoting particles) derived from the 'off' wavelength channel (313 nm). Despite the strong background from Rayleigh scattering at this short wavelength the light backscattered by the aerosols may, under typical PBL conditions, still be resolved with reasonable contrast. All examples shown in this paper are given as the ratio of the total backscatter coefficient, $\beta = \beta_P + \beta_R$, and the Rayleigh value, β_R (scattering ratio).

3.1.1. Warm season. Our results show that in summer the range with enhanced ozone and aerosol densities in our area may extend to more than 4 km a.s.l., i.e. 1 km above the maximum summit height. This is well above typical PBL heights outside the mountains and reflects the influence of the orographic wind system which is based on slope winds starting in the early morning, the (up-)valley wind building up at about 1000 CET (Central European Time, UTC + 1 h), enhanced convection and sometimes a compensating anti-valley wind above the PBL (e.g. Reiter et al., 1983; Müller and Reiter, 1986; Vergeiner and Dreiseitl, 1987). The vertical distribution is variable with the meteorological conditions and influenced by the complex orography in our area. A clear layer structure which would visualize the mechanisms of the different transport processes involved is not always seen.

In 1991, a major influence of summer-type photochemical ozone production could be observed as early as in March, when in the lower FT the mixing ratios were still near typical winter values (40 ppb). Figure 1a shows two vertical distributions of the O_3 mixing ratio selected from the series of 14 March. The presence of a high-pressure zone in the east of Central Europe implied advection from the south and rather high temperatures in the valley of about 16°C. At 830 CET the O_3 mixing ratio in the valley was rather low after significant night-time depletion. Between 1030 and 1640 CET the mixing ratio grew in the entire range up to more than 4 km a.s.l., in the lower PBL by more than 20%. For comparison, the values of the three nearby IFU stations Garmisch (730 m), Wank (1780 m) and Zugspitze (2940 m) are given and labeled in the sequence of the lidar measurements. They agree well with the lidar data, which is quite generally the case. It is, however, important to note that local ozone excursions in the vertical profiles typically not exceeding $\pm 7 \times 10^{-16}\,m^{-3}$ (about 3–10 ppb in the full vertical range of our system) are below the accuracy specifications for the lidar.

The expansion of the zone with enhanced ozone concentrations from about 3.2–3.7 km a.s.l. is qualitatively confirmed by the vertical profiles of the 313-nm scattering ratio (Fig. 1b). Until 1130

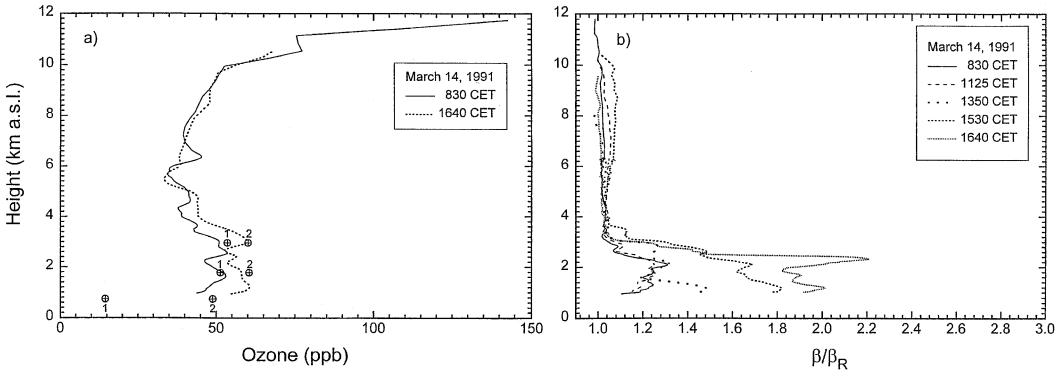

Fig. 1. Vertical distribution of ozone and aerosol from the measurements on 14 March 1991. (a) Ozone mixing ratio; the corresponding data of the IFU stations Garmisch (720 m a.s.l.), Wank (1780 m a.s.l.) and Zugspitze (2940 m a.s.l.) are marked by a circled cross. The tropopause height (Munich radio sonde) varies between about 11.0 (0000 UTC) and 11.5 km (1200 UTC). (b) Scattering ratio.

CET moderate aerosol concentrations were observed with β_P values amounting to about 25% of β_R and very few particles between 2.6 and 3.2 km. After a rather late onset of the valley wind more polluted air from outside the mountains was advected, starting at the bottom of the valley. As a consequence β_P gradually grew to values exceeding β_R. In the course of the afternoon, vertical transport reached up to 3.6 km (1530 CET). Near the end of the series at 1640 CET (about 1 h before sunset), the upper aerosol boundary lowered again and a very steep gradient formed at 2.5 km. This lowering is in pronounced contrast to the lidar and Zugspitze ozone data (continual concentration increase at 3 km until after midnight). This kind of discrepancy is not unique and has been repeatedly found.

A rather different case, not only related to the local orographic wind system, is shown in Figs. 2a and 2b, which contain ozone and aerosol profiles selected from the series of 15 June 1991. The weather situation around 15 June showed moderate high pressure reaching across the Alps from the Mediterrenean area. A front passed from the west to the east just slightly north of the Alps. Thus, advection from westerly directions prevailed in the lower troposphere. The maximum day-time temperature was about 22°C, which is clearly higher than that in the March case, but lower than normal.

The day-time variation of the aerosol distribution was not very pronounced, in contrast to the situation for O_3, for which all typical signs of vertical redistribution due to convection and photochemical production in the PBL are observed. Around sunset, very surprisingly, the upper aerosol layer boundary jumped to 4.7 km and an early-night ozone increase took place in the range between 1.2 and 3.7 km. This rise is confirmed by the station data. At the end of the lidar observation period (2245 CET) the maximum was not yet reached. The Zugspitze mixing ratio after midnight (70.7 ppb) seems to be announced by the isolated ozone peak at 2.6 km in the 2245-CET profile of Fig. 2b.

The late occurrence of this ozone concentration growth excludes local photochemical production as an explanation. The interpretation may be derived from the Zugspitze wind data. The wind direction flipped from west to south after 1830 CET, suggesting advection from Northern Italy where high ozone concentrations are known to form due to its large industrial and urban areas. At the same time, the wind speed continuously rose from 3.7 to 15.0 m s^{-1} (0030 CET), which qualifies the entire Po basin as the source area of the polluted air mass. Figure 3 shows two NOAA trajectories arriving at the Zugspitze summit at 1200 and 2400 UTC, respectively. The change in wind direction is confirmed, but not fully reproduced, which may be due to the model orography chosen for the Alps. The midnight trajectory follows the Central Alps between Switzerland and Italy. Given the measured wind direction we see this trajectory as the northernmost potential advection pathway. It should, nevertheless, be

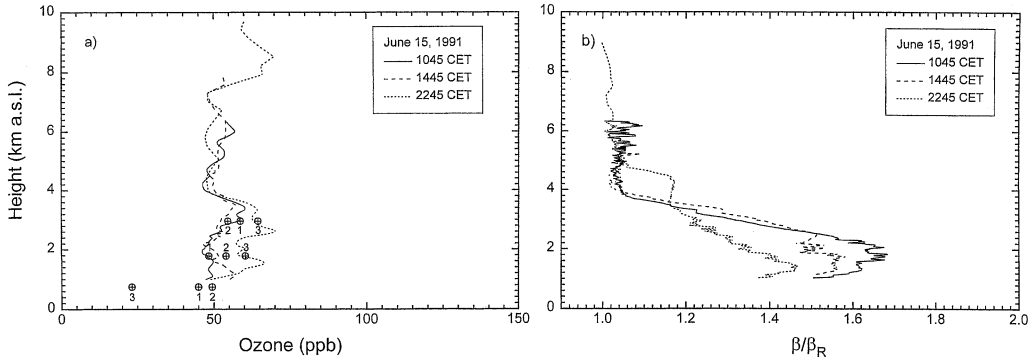

Fig. 2. Vertical distributions of ozone and aerosol from the measurements on 15 June 1991. (a) Ozone: the increase in mixing ratio after sunset is tentatively ascribed to trans-Alpine transport. The useful range is sometimes reduced due to the presence of low-lying cirrus clouds. (b) Scattering ratio: During the evening hours the aerosol layer expanded by approximately 1 km. The reduced quality of the data above 5 km a.s.l. is caused by low laser power.

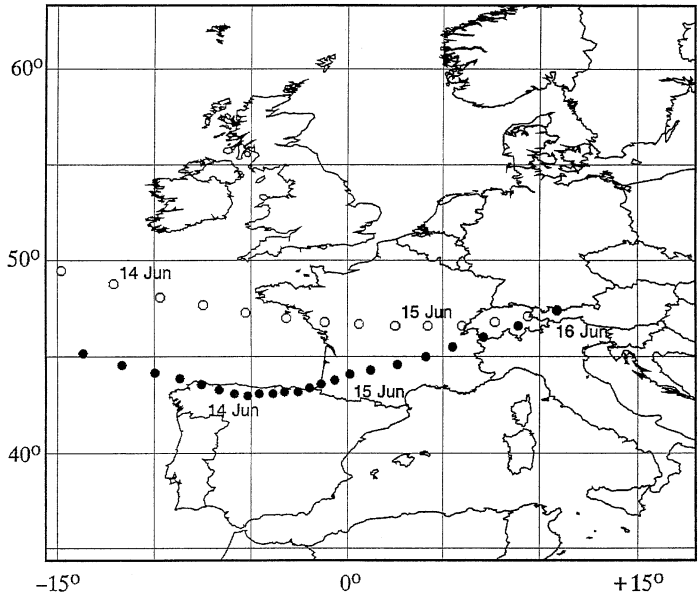

Fig. 3. Isentropic backward trajectories calculated by NOAA CMDL for the Zugspitze summit on 15 June (1200 UTC and 2400 UTC); neigbouring dots differ by three hours.

considered that Po-basin air pollution is sucked into the Alpine valleys by the day-time thermal wind and may flow all the way up to the Central Alps (see Section 4.1). In the upper part of the valleys it is lifted to considerable height and may be caught by the synoptic wind.

The example of 15 June provides another interesting observation. In the morning an ozone peak is visible which had formed at around 3 km a.s.l. during the preceding night. This peak gradually disappeared and a rather constant mixing ratio was finally reached above 1.6 km. The decreasing ozone mixing ratio is confirmed by the Zugspitze values, which declined from 63.3 to 53.6 ppb between 830 and 1530 CET. We ascribe this behaviour to the onset of vertical mixing. The Zugspitze record shows minor O_3 maxima also during the late hours of the preceding nights. A

cycle of night-time ozone maxima and day-time ozone reduction has also been known for other high-lying mountain stations (e.g. Kaiser, 1999). It is uncertain from our single example whether these maxima are always limited to a certain height range.

The most instructive example of the influence of the local vertical transport in the Alpine wind system was observed on 3 September (Fig. 4). Around this day Garmisch-Partenkirchen was located on the south side of a long high-pressure zone extending from the Atlantic ocean far beyond the Irish coast into Russia. As a consequence easterly winds prevailed which brought along continental air from East Europe.

In the morning a pronounced ozone maximum was present near 1.6 km a.s.l. A comparison of the 0755 and 0935 CET traces shows some ozone redistribution due to the onset of convection, the changes being nicely confirmed by the station data (Wank in particular). Later on, the valley wind carried polluted, ozone-loaded air into the valley. The mixing ratio finally reached in the valley (69.3 ppb at 1630 CET) exceeded that on the preceding day by 3.0 ppb, which would indicate the contribution of at least some photochemical ozone production. The puzzling isolated early-morning rise at the Zugspitze level (0935 CET profile) might be a partial revival of the high night-time values (67.8 ppb; both the upper-tropospheric weather maps and radio-sonde data suggest the presence of the wing of a stratospheric air intrusion).

The upward transport mechanism becomes more evident from an inspection of the aerosol data (Fig. 4b). In the range above 2.5 km a second aerosol layer was advected in the afternoon, consistently exhibiting lower scattering ratios than the PBL. The isolated aerosol tongue at about 3.5 km (1345 CET) arrived rather shortly after the onset of the valley wind. This suggests that the layer is due to upslope transport of the air in the valley along the slopes of nearby mountains in the south followed by reverse-flow formation near 3.5 km. The formation of an anti-valley wind requires weak interference by the synoptic wind in the lower free troposphere. In fact, the wind speed of the Munich radio sonde in that height range varied between just 0 and 3.6 m s^{-1}, the direction changing between east and south.

3.1.2. Winter. The maximum summer-time daily ozone production in our data ranges between 5 and 10 ppb. A negligible concentration growth might be expected for the dark season. Nevertheless, in winter the ozone mixing ratio in the PBL may occasionally be slightly higher than that in the FT. Figures 5 and 6 show examples from the series on 10 January and 20 February 1991, respectively. In both cases ozone values exceeding the FT values extend approximately up to the Zugspitze level, i.e. well above the typical winter PBL boundary height. The optically very thin aerosol distribution is limited to heights below 1.7 km on 20 February and is not discernible on 10 January.

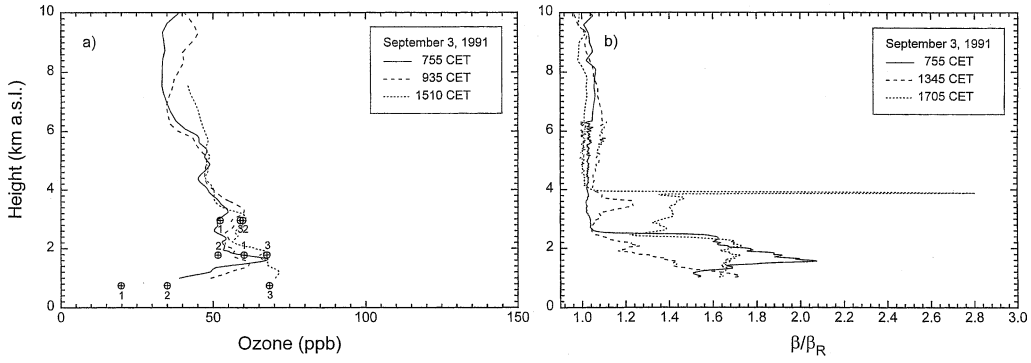

Fig. 4. Ozone and aerosol profiles from the series of 3 September 1991. (a) Ozone mixing ratio: The day-time increase above 2.2 km results from upward transport in the orographic wind system. The ozone drop above 6 km in the morning profiles is confirmed by a sonde ascent at Hohenpeißenberg. (b) Scattering ratio: near 1345 CET the first arrival of aerosol (at 3.5 km) returning from uplifting over nearby mountains is observed.

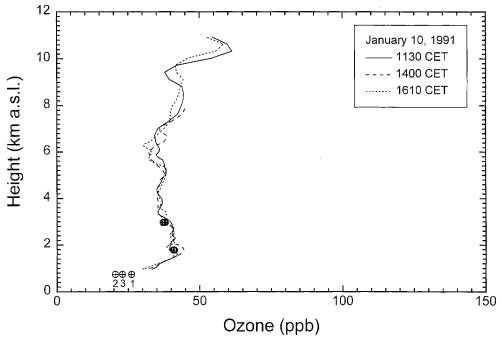

Fig. 5. Vertical ozone distributions on 10 January 1991; above the valley there is negligible variability of the mixing ratio throughout the day. The useful range is shortened by the presence of a thick layer of cirrus clouds above 10.7 km.

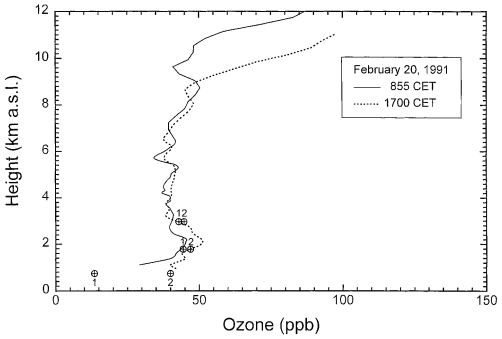

Fig. 6. Vertical ozone distributions on 20 February 1991; some indication of ozone build-up is seen up to the Zugspitze level. The Munich tropopause height changes from 12.5 km (0000 UTC) to 11.6 km (1200 UTC) and 10.1 km (2400 UTC). The lowering may be traced in both the 313-nm backscatter profiles and the ozone profile of 1700 CET.

In the case of the January example both the lidar and the station data reveal a negligible diurnal variation of the ozone mixing ratio. On 10 January, Garmisch-Partenkirchen was located at the north side of an extension of a huge Mediterrenean high-pressure zone implying potential advection from Switzerland and Southern France.

The high-pressure zone of 20 February was centred above the Black Sea. Thus, the advection pattern was different from that on 10 January, with winds arriving approximately from the south. On 20 February, some growth of the ozone mixing ratio took place starting at about 1300 CET. The southerly winds supported the warming during the day. Thus, limited vertical transport was possible. Indeed, the Wank NO_x mixing ratios exhibit a concentration increase during the late morning hours. In contrast, despite even higher temperatures at the Wank summit on 10 January, no comparable upslope transport was observed in that case. We doubt that upslope transport is responsible for the enhanced ozone all the way up to 3000 m, which suggests advection of ozone in warm air masses extending approximately up to that altitude.

3.2. Free troposphere

The mixing ratio of free-tropospheric ozone under high-pressure conditions in winter was found to be frequently rather constant as a function of height (Figs. 5 and 6). This is somewhat different in summer, when a higher variability of the vertical distribution is also seen, which is caused by more pronounced vertical exchange and advection. Particularly efficient vertical transport is expected to be caused by the orographically induced winds in and above the Alps (see Sections 3.1 and 4.1), which may be enhanced by the formation of clouds and thunderstorms. Further sources of inhomogeneous vertical distributions are intrusions of stratospheric air, advection of layers from source regions with rather different air pollution levels (see Sections 3.3 and 4.2) and the presence of layers with enhanced water-vapour concentrations (e.g. Weller et al., 1996; Kley et al., 1996; Reichardt et al., 1996).

There has been no evidence of reproducible diurnal cycles in the FT part of our vertical profiles. Unperiodic changes in the ozone distributions are quite frequently observed. In order to distinguish finer structures, particularly during the cold season, the accuracy of the lidar must be improved towards a level of a few per cent (see Sections 4.2 and 5).

Tables 1 and 2 lists our final average ozone mixing ratios for the different months in 1991 extracted for discrete heights (obtained by smoothing the values from the evaluated ozone profiles). The heights correspond to the boundaries of the range bins of the intercomparison exercise within TOR Task Group 1 (Scheel et al., 1997a, 1997b). The monthly mean values for the Zugspitze station and the Brewer-Mast

Table 1. *Monthly mean ozone mixing ratios (in ppb) from the lidar measurements in 1991 for the six heights (a.s.l.) limiting the height bins of TOR task group 1; the values are crude estimates based on just up to 3 measurement days per month*

Month	2500 m	3500 m	4500 m	5500 m	6500 m	7500 m
January	41.7	39.3	42.3	41.1	42.8	46.8
February	41.9	40.1	39.3	38.9	41.7	45.4
March	45.5	47.0	37.8	38.9	41.7	46.4
April	52.4	51.9	50.0	46.8	48.0	49.9
May	55.0	53.6	53.3	52.9	53.9	53.9
June	55.7	60.0	54.1	55.7	58.3	57.4
July	56.3	61.2	54.1	52.5	59.7	60.9
August	57.2	58.8	55.5	52.5	57.5	58.9
September	53.9	52.5	50.4	50.4	52.4	58.2
Oktober	43.6	47.6	49.9	51.8	50.9	55.0
November	42.0	41.8	48.2	48.6	48.7	50.3

Table 2. *Monthly mean values of the ozone mixing ratio provided by the Hohenpeißenberg observatory (MOH), averaged over the three height bins proposed for the intercomparison within Task Group 1 of the TOR project; for comparison, the Zugspitze data and the average of the lidar values for 2500 and 2500 m is given*

	Lidar 3000 m	Zugspitze 2940 m	MOH 2500–3500 m	MOH 4500–5500 m	MOH 6500–7500 m
January	40.5	41.8	41.7	45.0	47.6
February	41.0	42.6	39.1	47.7	60.0
March	46.3	47.2	46.3	49.9	53.7
April	52.2	54.9	49.6	52.0	56.5
May	54.3	51.3	53.3	62.6	70.8
June	57.9	52.0	54.1	60.6	72.3
July	58.8	57.8	59.0	64.8	72.3
August	58.0	56.0	52.5	59.7	66.4
September	53.2	52.5	49.4	49.3	53.5
Oktober	45.6	43.4	48.2	53.1	59.0
November	41.9	41.6	40.3	43.7	44.7
December		39.7	40.5	44.6	48.1

sounding of the Meteorological Observatory Hohenpeißenberg (Claude, 1995; Scheel et al., 1997a), which is located just 38 km north of our institute, are also included for comparison. The agreement of the lidar results with those from Wank and Zugspitze is astonishingly good taking into consideration that lidar profiles were evaluated for just a few days per month. In the upper troposphere the lidar data are consistently lower than the Hohenpeißenberg monthly means during the summer months. This discrepancy is discussed in more detail in Section 4.2.

3.3. Frontal passages and long-range transport

In this section we give one example of the temporal evolution of the ozone distribution after a frontal passage. In the majority of such cases aged, polluted continental air is replaced by cleaner marine air masses. Consequently, the ozone densities in the PBL are expected to be lowered and to approach the FT values. Afterwards, as soon as the advection of polluted air is resumed a rather quick build-up of elevated O_3 concentrations starts. This is a rather simplified view, in particular if the frontal passage leads to

the onset of anticyclonic conditions during the warm season. A complex layer structure may be observed in such cases (Eisele et al., 1999; Stohl and Trickl, 1999, 2000) and the episode described in the following (1–3 July 1991) is our first example giving some evidence of this behaviour. The main reason for selecting this episode from the 1991 cases was that two days of vertical profiles are available, including our first full 24-h series (2–3 July). The ozone concentrations were highly variable almost until the end of the observation period and reflected the influence of a number of different transport processes.

Following a cold-front passage, showers lasted until 30 June. On 30 June, a shallow high-pressure zone started to move across the Alps near the ground, whereas the map for the 500 mbar pressure level shows a persisting flow from the northwest (Figs. 7 and 8).

Figures 9–11 show selected vertical ozone and aerosol profiles from 1 July to 3 July 1991, together with the corresponding ozone values of the three IFU stations. Due the considerable temporal variability, which is expected to imply also some spatial variability, the agreement between the lidar and the stations is not always as satisfactory as usual. However, all concentration changes seen in the lidar results are qualitatively reproduced. It should be mentioned that over 48 h no significant average bias of lidar and station data may be resolved, given an overall standard deviation of 6%.

The low aerosol backscatter coefficients next to the ground and the moderate, background-type ozone mixing ratio of the order of 50 ppb throughout the troposphere at the beginning of the observations support the idea of an advection of clean air behind the front. However, in the course of the measurements several layers with different aerosol and ozone concentrations were distinguished which are described in the following. The air masses in the layers are characterized by radiosonde data and ten-day backward trajectories for 3 km, as well as for 4 and 5 km (recently calculated on request).

Layer 1 (PBL, up to about 2.5 km). The ozone mixing ratio and the aerosol backscatter ratio in

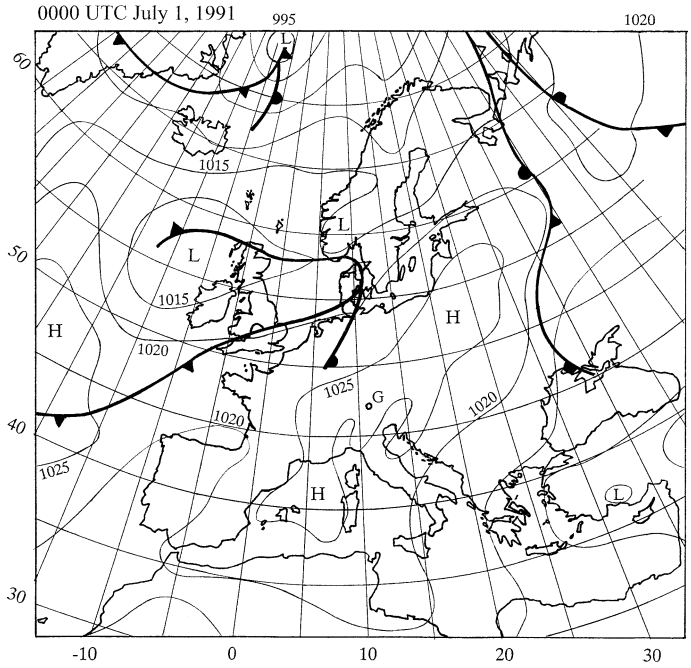

Fig. 7. 1000-mbar weather map for 0000 UTC on 1 July 1991; the geographical co-ordinates are given in degrees, the pressures of the isobars in millibars (source: Deutscher Wetterdienst, DWD).

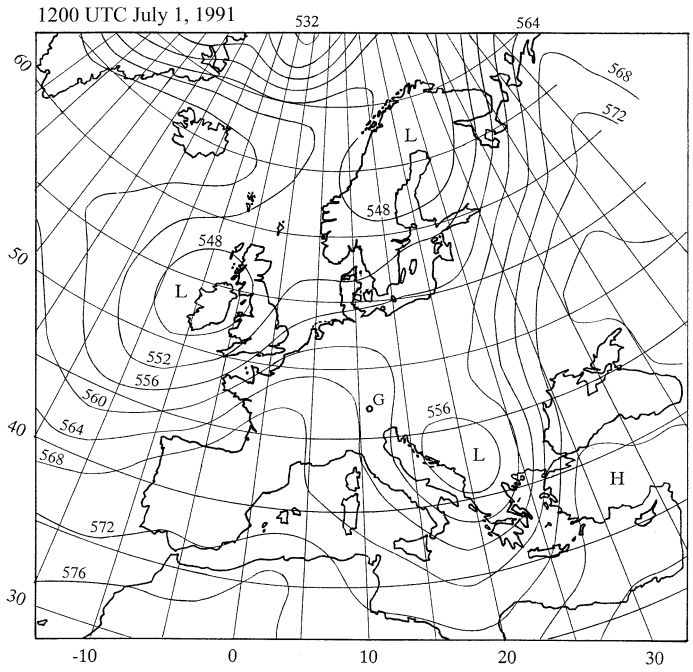

Fig. 8. 500-mbar weather map for 1200 UTC on 1 July 1991; source: DWD.

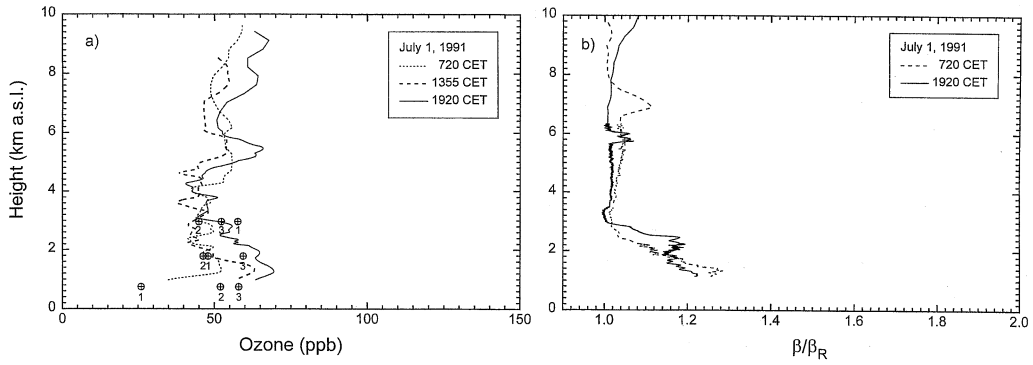

Fig. 9. Vertical distributions of ozone and aerosol from the series of 1 July 1991, obtained during the period following a cold-front passage. (a) Ozone mixing ratio. (b) Scattering ratio: the broad shape of the aerosol peak at about 7 km is caused by averaging the data in 300-m intervals above 6.3 km (photon-counting resolution).

the PBL were highly variable, with pronounced deviations from the typical diurnal variations. On 2 July the aerosol completely disappeared between about 0900 CET and noon. The variations of the ozone concentration substantially slowed down during the first hours of 3 June (Fig. 11). This indicates that the lower troposphere above our area was now filled with polluted continental air.

Layer 2 (around 3 km). This layer is characterized by a vertically isolated ozone peak which repeatedly formed at about 3 km a.s.l. (see morning examples in Figs. 9a and 10a). Its occurrence during the morning hours and its separation from the PBL suggests that it was caused by horizontal advection rather than by vertical transport in the Alpine wind system. The Zugspitze ozone data

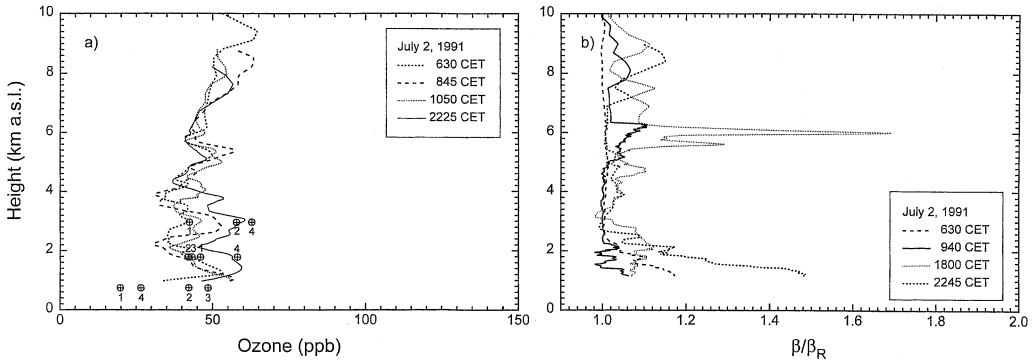

Fig. 10. Vertical ozone and aerosol distributions from 2 July 1991. (a) The variability of the ozone mixing ratio was similarly high as on the preceding day. (b) Scattering ratio.

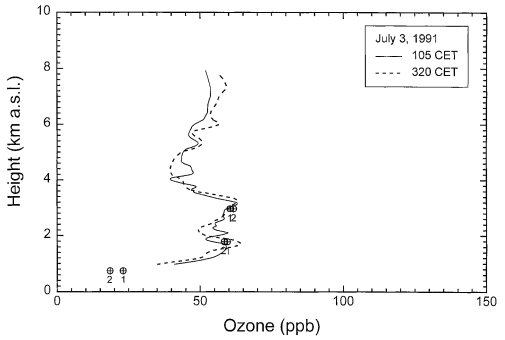

Fig. 11. Ozone profiles from the second part of the night between 2 July and 3 July 1991; the variability of the ozone mixing ratio observed earlier has stopped due to a longer residence time of the air over the continent.

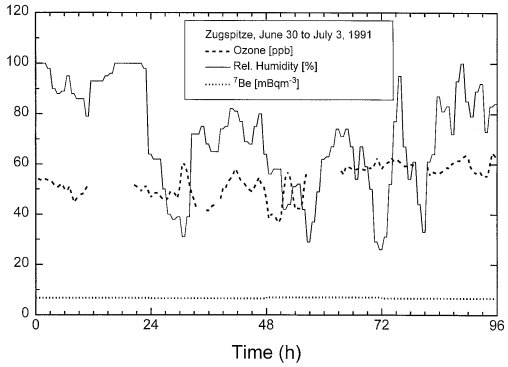

Fig. 12. Time series of ozone mixing ratio, relative humidity and ^{7}Be for the Zugspitze station between 30 June and 3 July 1991; the five humidity dips are most likely caused by long-range advection of stratospheric air.

(Fig. 12) show the temporal evolution of this layer in more detail. All three morning peaks in Fig. 12 occurred simultaneously to relative-humidity dips to values below 40%. Two more humidity dips followed on 3 July (0000 and 0900 CET), when the elevated, but more or less constant ozone level reflects a more continental nature of the air. The elevated ^{7}Be values and the trajectories suggest the presence of aged stratospheric layers during the humidity-dip phases, corresponding to rather different intrusion areas in the Arctic above 60°N. The trajectories which do not correspond to a humidity dip originate over the Atlantic Ocean between 30 and 40°N, which explains the moderate ozone values. They approach anticyclonically with northernmost points over England, with increasing residence time over the continent in agreement with our above conclusion.

Layer 3 (up to about 4 km). The ozone mixing ratios in layer 3 range between 30 and 45 ppb. The trajectories for 4 km show the air parcel over the central Atlantic between 20 and 30°N 10 d backward in time. A mixing ratio of the order of 30 ppb was, indeed, reported by Weller et al. (1996) for latitudes below 30°N.

Layer 4. The ozone profiles on 1 July show a distinct peak in the afternoon which slowly descended from 5.5 km at about 1400 CET (first observation) to 4.9 km at 2100 CET. The weather map in Fig. 8 suggests pronounced anticyclonic bending of the jet stream over Central Europe and thus the occurrence of a stratospheric air intrusion. However, the profiles of the nearestby

radio-sounding stations, Stuttgart and Munich in South Germany, do not indicate any dry layers. In the west, the data from Payerne (Switzerland) and the French stations exhibit all signs of a pronounced stratospheric intrusion. Our results suggest at least a part-time passing of the eastern edge of the intrusion over Garmisch-Partenkirchen.

Layer 5 (mid-tropospheric aerosol). The stratospheric layer on 1 July was topped by a thin aerosol tongue which was visible during the first three and final five hours of the measurement period (0720–2100 CET) and subsided from 7.1 to 5.6 km (Fig. 9b). The observation of aerosol above a layer of stratospheric origin is interesting and deserves a few more words. On 1 July the first observation of the Pinatubo volcanic plume above IFU took place (Jäger, 1992). Our measurements at 313 nm show an intense Pinatubo aerosol peak varying in height between 14.2 km in the morning and 15.0 km in the evening. Since Browell et al. (1987) found volcanic aerosol in a tropopause fold in the case of the El Chichon eruption a similar mechanism might be concluded here. However, the puzzling fact that the aerosols are located at the top of the ozone tongue suggests one should look for another possibility.

The descending aerosol layer on 1 July could also be identical to the mid-tropospheric layer on 2 July, although these structures are substantially wider and are at least shortly interrupted as may be concluded from the measurement of 0630 CET on 2 July (Fig. 10b). The aerosol contributions to the signal were mostly very low and clearly below any expectations for clouds (which should not have occurred because of a moderate free-tropospheric humidity). A somewhat higher aerosol signal was observed in the period 1600–2030 CET.

The aerosol layer on 2 July was traced back to the east coast of the United States near 30°N (3.5–4.0 km a.s.l.) by the trajectories for 5 km a.s.l.. The air was lifted to about 6 km in or in the vicinity of the cold front shown in Fig. 7 and anticyclonically subsided by 1 km during the final travel day. An explanation of the aerosol structures seen on 2 July could therefore be intercontinental transport. The peak ozone mixing ratio in the corresponding height range, 60 ppb, is somewhat high for purely marine air from lower latitudes, which would support the idea of advection from the southern USA.

Extensions of the 5-km trajectories for 2 July by another 10 d lead to two different areas, Los Angeles (0000 UTC trajectory) and the sea south of Cuba (1200 UTC trajectory). The TOMS (Total Ozone Mapping Spectrometer) aerosol data (http://toms.gsfc.nasa.gov) show enhanced aerosol in both areas, but nowhere else in the southern US. The Caribbean aerosol layer is fed by an enormous particle tongue starting in the Persian Gulf (1991 oil fires), as identified by the sequence of satellite images. The concentrations reached the TOMS scale maximum over most of the Sahara desert and Arabia in May and June, far beyond typical mean aerosol levels in this region. A large-scale fire as the source could explain the highly chaotic structure of the mid-tropospheric layers above our site. The long survival of the structures (and layers) is an interesting observation and stimulates further work.

3.4. Föhn

Föhn is formed if air traverses the Alps from the south, typically at the end of a high-pressure period or in the presence of a warm front arriving from the south-west. The consequence is a considerable temperature increase and relatively dry air on the north side of the mountains.

A case of Föhn with long-range advection is described in the following (11 October 1991). The weather situation for 11 October is depicted in Fig. 13. Along a front extending as far as North Africa dry and warm air from the Sahara desert was blown all the way up to our latitude. A temperature increase of about 4°C was registered at the Zugspitze station, together with reduced visibility due to the dust particles from the desert. The lidar data revealed enhanced aerosol up to 3.7 km, a minor portion for some time up to 5 km, in agreement with the more extensive measurements by Jäger et al. (1988).

The aerosol backscatter coefficients retrieved from the 313-nm lidar signals range within less than 20% of the Rayleigh backscatter coefficients, in some conflict with the more pronounced lowering of the visibility at the Zugspitze summit (measured at 550 nm). This discrepancy is explained by the strongly enhanced Rayleigh scattering in the UV and the low wavelength depend-

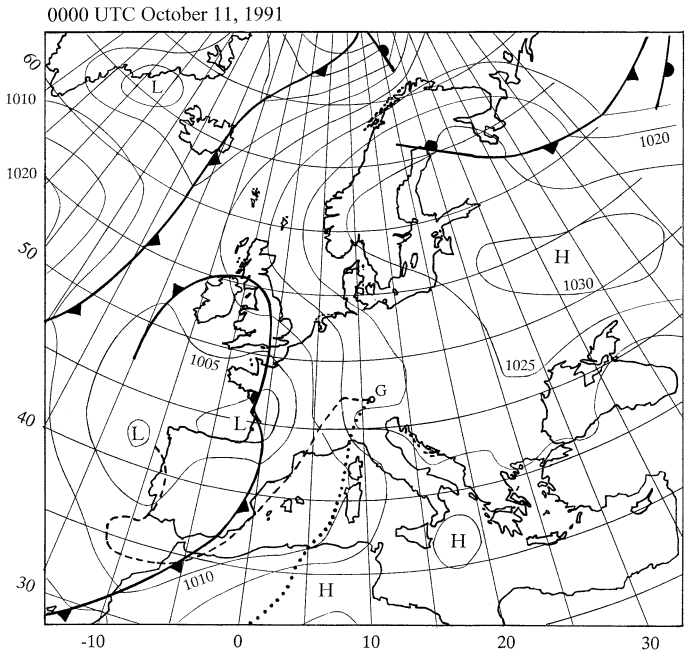

Fig. 13. Weather map for 11 October 1991 (0000 UTC; source: DWD); two NOAA CMDL backward trajectories, arriving at the Zugspitze summit at 0000 UTC (dashed line) and 1200 UTC (dotted line) are inserted to show the transition from more westerly advection to Föhn within this period of time. The 0000 UTC trajectory is displayed for six days.

ence of the light backscattering by the large (Jäger et al., 1988) Saharan-dust particles. Assuming a $\lambda^{-1.5}$ wavelength dependence of β_P, which we have most frequently applied to correct the aerosol-induced ozone density errors (Kempfer et al., 1994), the ozone densities below 3.5 km are underestimated by about 10%. A λ^0 dependence, as expected for large particles, yields a much better agreement with the Wank and Zugspitze values and was, consequently, applied.

Figure 14 shows the results of two ozone measurements on 11 October at 0845 and 1640 CET. The two distributions reveal astonishingly low ozone values of the order of 35 ppb throughout the troposphere. Below 1.5 km the values remarkably dropped during the period of observation (until 1800 CET). The ground-level values on 11 and 12 October typically ranged between 15 and 2 ppb and did not exhibit the typical late-morning rise to upper-PBL values, indicating ongoing O_3 destruction at the surface due to the Föhn rotors. The lidar data show a vertical growth of the depleted layer during the day.

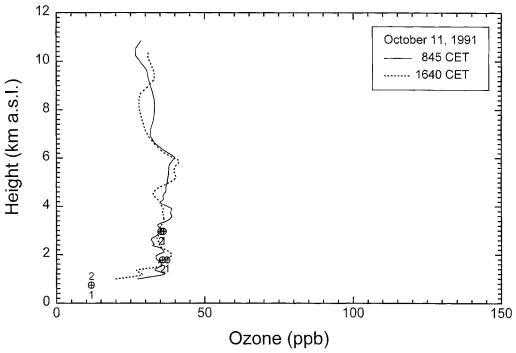

Fig. 14. Two ozone profiles during the Föhn episode of 11 October 1991; the mixing ratio is very low due to air advection from latitudes near 20°N.

Sections of two 10 d backward trajectories for the Zugspitze summit are included in Fig. 13. The noon trajectory starts at 24°W 10 d before it intersects our area. For the entire period of approach towards the African coast the air

travelled between 18 and 22°N, which explains the low mixing ratios (see Section 3.3).

4. Discussion

The examples given in Section 3 show that a lot of details may be extracted from combined lidar and station measurements. Some interpretation of the individual examples has already been given. In the following we discuss the more general aspects.

4.1. Boundary layer

The lidar data agree well with the results of the extensive ozone measurements onboard the cable car between Eibsee (990 m a.s.l.) and Zugspitze (Reiter et al., 1987; Reiter, 1990), which reveal typical ozone mixing ratios between 60 to 80 ppb in the height range below the Zugspitze summit in summer [which remained approximately at the same level between 1983 and the late 1990s (Scheel et al., 1999)]. The lidar measurements take place far away from the slopes and should be less sussceptible to ozone deposition effects during periods of strong slope winds. However, their principal advantage is that they yield additional information on the range above 3000 m, which was found not to belong exclusively to the FT in many cases. This fact, which is very important for the data selection for high-lying monitoring stations, had not been that obvious before the beginning of this work.

A lot of our interpretation is based on IFU research in the 1980s. Under high-pressure conditions in summer an orographic wind system builds up between the Alps and the area outside the mountains (Reiter, et al., 1983). In the late morning an up-valley flow forms next to the ground (valley wind). It was shown that the morning rise of O_3 in the bottom section of the valley is not predominantly caused by the advection of polluted air masses from outside the Alps after the build-up of the valley wind (Reiter et al., 1987). An investigation with stations distributed along the valley over a distance of 20 km revealed that there is no time delay of the daily ozone rise at the different stations. The vertical soundings show that this coincidence is due an early beginning of vertical exchange which precedes the full build-up of the valley wind. Photochemical ozone production cannot account for the entire pronounced concentration increase observed at the ground every day, after an almost complete removal over night. From our data we conclude a typical effective production rate of 5–10 ppb per day in the PBL, in agreement with examples found in the literature [for a more complete discussion see, e.g. (Fishman et al., 1985)]. Photochemistry tends to create O_3 preferentially in the lowest layer where most of the advected air pollution is concentrated (Figs. 1a, 2a and 4a).

The main nearby source of air pollution is the city of Munich. Transport from the Munich area into the Alps could proceed within less than 10 h when assuming wind speeds of more than 2 m s^{-1}. However, although the attraction by the valley wind reaches far outside the mountains there is no clear evidence that the Munich plume may be accessible before it expands to a sufficient size. There is also some indication that elevated ozone concentrations at our site may be related to an extended residence time of the advected air over a larger part of the continent (see Section 3.3).

The upward transport in the orographic wind system, which lifts the PBL air to heights beyond 1 km above the summits and crests, is highly efficient and may contribute quite considerably to the PBL-FT transport, at least if one assumes subsequent transport outside the mountains and mixing into the FT over the lower-lying terrain. The efficiency is demonstrated by the not very significant lowering of the aerosol density during the upward transport which is mainly due to the widening of the valley with growing altitude (Fig. 2b). In higher regions of the Alps aerosol transport to at least 4.45 km a.s.l. has been reported (Lugauer et al., 1998). Considering the large area of the Alps we expect that the Alpine contribution to the pollution export from the PBL should clearly exceed that above flat terrain which was evaluated by the TOR vertical-exchange task group (Beck et al., 1997). More concentrated efforts to evaluate the orographically induced transport in the Alps have been started in 1996 as a part of the VOTALP project [Vertical Ozone Transport in the Alps; (VOTALP, 2000)]. A field experiment carried out in the Swiss Mesolcina valley yielded upward transport efficiencies of the order of 80% which confirms our above conclusions (Carnuth and Trickl, 2000; Furger et al.,

2000). As in the case of Fig. 4b, bimodal aerosol distributions were observed. The upper step in that distribution could be associated with a reversed wind direction by aircraft-based measurements. The very deep structure of the Mesolcina valley (300 m to about 3000 m) is favourable for observing a wind reversal due to some channeling. The valley structure near Garmisch-Partenkirchen is rather open above 1800 m, and thus more exposed to the synoptic wind. All observations of bimodal aerosol distributions in recent years could be attributed to low synopic wind speeds and wind directions in the sector east to south. It is planned to combine the lidar studies with aircraft-based wind measurements to obtain information on the coupling between the rising air streams and the synoptic wind.

The measurements in the Mesolcina valley also give some hint on the mechanism underlying the episode of trans-Alpine transport on 15 June 1991 (Section 3.1). The polluted air from the Po basin penetrates the Alpine valleys and may even reach the Central Alps. Again, the typical upper transport boundaries were found at about 1.5 km above the surrounding summits (Carnuth and Trickl, 2000), also in some agreement with the night-time aerosol profile in Fig. 2b.

An increase of the ozone concentration due to trans-Alpine transport would, in general, be expected for Föhn episodes. One example showing such a concentration rise was recently studied within the VOTALP project. The values reached 80 ppb on the north side of the Central Alps for the first few hours after the beginning of the Föhn event (Seibert et al., 2000). A climatological study in that paper shows that there is a general tendency for such an ozone increase during Föhn. However, the Sahara-dust episode described in Section 3.4 suggests that high ozone concentrations are less likely to occur if prefrontal long-range transport from low latitudes to our area is involved. Low O_3 concentrations at the Zugspitze summit have mainly been associated with advection from low latitudes (Scheel et al., 1993, 1998).

During night-time the wind system is reversed [8 p.m. to 8 a.m. (Reiter et al., 1983)]. Cold air from the central part of the Alps or the free troposphere slides down the slopes and forms the so-called mountain wind in the valley. As a result of the enhanced deposition forced by this downhill wind a particularly pronounced ozone loss is observed next to the ground (Broder et al., 1981; Broder and Gyax, 1985). The lidar results confirm that the ozone depletion is confined to a rather shallow layer next to the ground. However, day–night oscillations of the ozone concentration are not restricted to complex terrain with a thermally driven wind system. Kelly et al. (1984) concluded that dry deposition of ozone is the dominating night-time ozone-depleting mechanism in rural areas with low NO concentrations. They suggested the presence of a low-lying nocturnal inversion layer to be responsible for the enhanced deposition in the cases discussed in their publication.

Winter-time ozone concentrations below 3000 m above the free-tropospheric values in the presence of advection have also been found in the case of the cable-car investigations (Reiter, 1990). Although the photochemical ozone production is reduced by one order of magnitude in winter, the long life-time of the relevant constituents during the cold season can lead to ozone production, as long as night-time chemistry does not prevail (Liu et al., 1987).

4.2. Free troposphere

Valuable information on the lowest part of the atmosphere may to be provided by mountain-based stations. However, the ozone distribution in the true FT, which may start even well above the Alpine summit level in summer, is only accessible by vertical sounding. The advantages of the lidar method should be seen in concentrated investigations of selected episodes, although trend studies should also be attempted and compared with the results of balloon stations. This is an attractive goal since, due to the low aerosol density in the FT, in principle an accuracy next to that of the absorption cross-section of O_3 (which is 1% and better) may be reached. Although the results of this study do not come close to this, the seasonal variation of the 1991 data was evaluated.

Tables 1 and 2 (Section 3) list the seasonal variation for discrete heights in the FT. As pointed out in Section 3, the agreement of the 'monthly mean' values in the tables with the monthly mean values of Wank and Zugspitze is excellent, despite the fact that only a few days of lidar measurements per month have entered this analysis. In particular, after August 1991 the days on which data were taken became more and more sparse. Within the

FT the lidar data may be compared to the results from Brewer-Mast soundings at Hohenpeißenberg, which is located 38 km in the north of IFU. The 1991 monthly means of the Hohenpeißenberg observatory (Claude, 1995) are consistently higher in the FT. This discrepancy is particularly pronounced during the summer months (up to -15 ppb).

There have been discussions about the quality of ozone-sonde data within the troposphere. However, the Hohenpeißenberg sonde data were carefully re-analysed (Köhler, 1995; Schwarz and Steinbrecht, 1996; Steinbrecht et al., 1998). The treatment has lowered the tropospheric mixing ratios with respect to those published earlier (MOH, 1992; see also Beekmann et al., 1994a). As one can see from Table 1 the Zugspitze monthly means (2.96 km) and the 2.5–3.5-km averages for the Hohenpeißenberg sonde for 1991 now agree to within ± 3.7 ppb. The IFU lidar was successfully validated by ECC-sonde ascents and a comparison with an aircraft-based ozone profile (Kempfer et al., 1994). Without an appropriate correction typical systematic lidar errors (Section 2.2) may, indeed, yield lower O_3 values in the uppermost part of the useful range. However, the evaluation procedure applied to our 1991 measurements even tends to generate a slighty higher ozone mixing ratio in the correction-sensitive uppermost 2.5 km than in the lower FT and not the opposite. This was judged mostly from the profiles for the cold season (e.g. Figs. 5 and 6), which are more likely to exhibit a rather constant mixing ratio than those for the summer months.

We conclude that the pronounced negative deviations of the average values in summer are due to not routinely taking data on days with enhanced ozone concentrations between 5 and 10 km. Recent results have shown that even the 'ozonopause' may occasionally sink to heights below 8 km which should substantially influence the mean concentrations (Eisele and Trickl, 1998; Eisele et al., 1999). In fact, the summer maximum (August mean value) in our 1996 annual series was 80 ppb due to focussing on an investigation of stratospheric air intrusions (Eisele, 1997). Also long-range transport was recently shown to result occasionally in a substantial ozone increase in the mid and upper troposphere during the warm season (see below).

The pronounced annual cycle of O_3 in the FT may been seen to be a consequence of anthropogenic emissions and vertical transport (e.g. Logan, 1985; Volz and Kley, 1988; Volz et al., 1989). Both upward transport of O_3 from the boundary layer and upward transport of precursors with subsequent photochemical ozone formation have to be taken into consideration. Pickering et al. (1990) conclude that the photochemical ozone production dominates over destruction in the entire troposphere above the central United States. In addition, if an elevated amount of non-methane hydrocarbons is promoted to the FT (e.g. in clouds) a significant increase of the ozone-production potential is derived in a model analysis of their experimental data. They also demonstrated the importance of thunderstorms and lightning for NO_x production and the ozone chemistry in the upper troposphere (see also Liu et al., 1983; Höller et al., 1999 and references therein). Hydrocarbon mixing ratios of at least a few ppb are reported for the mid-latitude FT in the vicinity of continents in the northern hemisphere (e.g. Rudolph, 1988; Singh et al., 1988; Rudolph, 1995). As to NO_x a threshold for ozone production near 0.1 ppb is suggested (Lin et al., 1988; Stockwell et al., 1996). Measured NO and NO_2 mixing ratios in the continental FT are reported to be both near this value (e.g. Drummond et al., 1988). Model results cited by Beekmann et al. (1994a) indicate that even 2.0–2.5 ppb of ozone should be produced in the middle FT per day from the precursors exported from the PBL.

Quite differently from our findings, lidar measurements at a TOR station next to the German coast, strongly influenced by marine air, have not shown a clearly discernible seasonal variation of the ozone concentration in the lower FT beyond some indication of a springtime maximum (Bösenberg et al., 1997). Nevertheless, the average mixing ratio in the lower FT is as high as 50 ppb, reflecting some anthropopgenic contribution. This observation could suggest that most of the excess O_3 seen in our summer FT data is produced over the European continent rather than caused by advection from outside Europe. On the other hand, Jacob et al. (1993) conclude that 70% of the 'pollution O_3' from North America is exported. The model calculations showed that this export takes place in the FT, to a major part promoted by upward transport due to the mountains.

Investigations of significant transport of ozone and carbon dioxide out to the Atlantic ocean were reported on by Parrish et al. (1993) and Fehsenfeld (1994). Due to the long lifetime of O_3 in the FT, the North American contributions, together with those from all the other highly industrialized areas, should form a measurable part of the background ozone concentration in the FT. The absence of a clear summer ozone maximum in the lower FT at the German coast indicates a substantial modification of the air composition in the lower troposphere over the remote North Atlantic.

Measurements published in recent years suggest a principal transport pathway for North-American air pollution at higher altitudes (e.g. Fehsenfeld et al., 1996; Wild et al., 1996; Arnold et al., 1997; Penkett et al., 1998; Bethan et al., 1998). Indeed, elevated ozone values (80–110 ppb) in the upper troposphere seen in one- to four-day series of lidar measurements at our site by Eisele et al. (1999) in 1996 and 1997 could, in part, be traced back by trajectory calculations to the boundary layer of the United States (Stohl and Trickl, 1999, 2000). Intercontinental transport may contribute to the complexity of starting anticyclonic episodes such as that described in Section 3.3. The existence of a detailed layer structure during such episodes, with contributions from rather different areas of the northern hemisphere and ozone mixing ratios between 30 and more than 100 ppb, makes the definition of an ozone background level a difficult task.

5. Conclusions

The examples discussed in this paper demonstrate the importance of wide-range ground-based lidar sounding for tropospheric ozone studies. Under cloud-free or partly cloud-free conditions dense time series may be carried out and allow the different processes contributing to the vertical profiles to be distinguished. Our lidar, combined with the local station network, which covers an altitude range up to 3000 m a.s.l., trajectory analyses and, as a future perspective, concentrated aircraft flights, offers an excellent basis for quantitative investigations.

As expected, the soundings show the typical day-by-day growth of the ozone concentration in the presence of sufficient sunshine. However, most information obtained is related to the influence of transport. Efficient upward transport of ozone and aerosols takes place in the Alpine wind system. For moderate humidity the PBL air is lifted to heights between 1 and 1.5 km above neighbouring summits. Vertical exchange over the Alps is expected to yield a significant contribution to the PBL-FT exchange in this part of Central Europe. It is obvious that aerosol is a better tracer for vertical-exchange studies than ozone. Further studies related to vertical transport in the Alps have recently been carried out and will continue during the next few years focussing on the coupling of the Alpine thermal wind system to the synoptic wind. The necessary information on the wind field will be derived from aircraft measurements.

In addition to the local transport medium- and long-range advection was studied. In particular, an ozone increase most likely due to the arrival of polluted air from Northern Italy, very low mixing ratios during a Föhn episode, for which trajectories could be traced back beyond the Sahara desert to the central part of the Atlantic Ocean, and the development of the ozone distribution after a frontal passage with inflow of marine air from the North and Central Atlantic are documented. The latter cold front led to anticyclonic conditions during which a rich layer structure could be observed almost simultaneously. The different layers corresponded to direct and aged stratospheric air intrusions, air from latitudes below 30°N with an ozone mixing ratio of the order of 40 ppb and, very likely, input from North America. The latter air mass might also have contained contributions from the Kuwait oil fires in 1991. This kind of vertical structure was repeatedly observed during the onset of anticyclonic conditions in recent years. It is therefore not a good idea to associate a frontal passage with the exclusive advection of clean marine air masses. A key task of the TOR project was to determine the European modification of the background ozone concentration. We have started to put another question: Can such a background level be defined?

The studies have also shown that meaningful tropospheric ozone studies require an operating range from next to the ground level into the lower stratosphere at an accuracy level of just a few per cent. The necessary lidar upgrading to three-wavelength operation with improved spectral filtering could finally be started in 1995 (Eisele and

Trickl, 1997). As a consequence, the vertical range of the lidar could be extended to heights 3–5 km above the tropopause, with ozone errors of the order of 5%. The measurements may now be carried out under automatic control and have been extended to four days.

6. Acknowledgements

We thank W. Seiler for stimulating and supporting this work. H. E. Scheel and R. Sladkovic kindly supplied the data of the nearby IFU stations and made valuable suggestions. Most information on earlier work on the Alpine wind system has been contributed by H. Müller. Discussions with the members of the TOR community are gratefully acknowledged. We also thank J. Harris and E. Rice (NOAA CMDL) for providing the isentropic trajectories and G. Smiatek for generating the trajectory plot shown in Fig. 3. Until March 1991, this work was funded by the German Bundesministerium für Forschung und Technologie under contract 07EU710/4.

REFERENCES

Ancellet, G., Pelon, J., Beekmann, M., Papayannis, A. and Mégie, G. 1991. Ground-based lidar studies of ozone exchanges between the stratosphere and the troposphere. *J. Geophys. Res.* **96**, 22,401–22,421.

Ancellet, G., Beekmann, M. and Papayannis, A. 1994. Impact of a cutoff low development on downward transport of ozone in the troposphere. *J. Geophys. Res.* **99**, 3451–3468.

Ancellet, G. and Beekmann, M. 1997. Evidence for changes in the ozone concentrations in the free troposphere over southern France from 1976 to 1995. *Atmos. Environ.* **31**, 2835–2851.

Ansmann, A., Neuber, R., Rairoux, P. and Wandinger, U. (eds.) 1997. *Advances in atmospheric remote sensing with lidar. Part V, tropospheric trace gases and plumes.* Springer, Berlin, Germany, 351–478.

Arnold, F., Schneider, J., Gollinger, K., Schlager, H., Schulte, P., Hagen, D. E., Whitefield, P. D. and van Velthoven, P. 1997. Observation of upper tropospheric sulfur dioxide and acetone pollution: potential implications for hydroxyl radical and aerosol formation. *Geophys. Res. Lett.* **24**, 57–60.

Beck, J. P., Asimakopoulos, N., Bazhanov, V., Bock, H. J., Chronopoulos, G., De Muer, D., Ebel, A., Flatøy, F., van Haver, P., Hov, Ø., Jakobs, H. J., Kirchner, E. J. J., Kunz, H., Memmesheimer, M., van Pul, W. A. J., Speth, P., Trickl, T. and Varotsos, C. 1997. Exchange of ozone between the atmospheric boundary layer and the free troposphere, Final Report of TOR Task Force 3a. In: *Transport and chemical transformation of pollutants in the troposphere, Final Report of the EUROTRAC Project, vol. 6, Tropospheric ozone research* (ed. Ø. Hov). Springer, Berlin, Germany, 111–130.

Beekmann, M., Ancellet, G. and Mégie, G. 1994a. Climatology of tropospheric ozone in southern Europe and its relation to potential vorticity. *J. Geophys. Res.* **99**, 12,841–12,853.

Beekmann, M., Ancellet, G., Blonsky, S., De Muer, D., Ebel, A., Elbern, H., Hendricks, J., Kowol, J., Mancier, C., Sladkovic, R., Smit, H. G. J., Speth, P., Trickl, T. and Van Haver, P. 1997a. Regional and global tropopause fold occurences and related cross-tropopause ozone flux. *J. Atmos. Chem.* **28**, 29–44.

Beekmann, M., Ancellet, G., Blonsky, S., De Muer, D., Ebel, A., Elbern, H., Hendricks, J., Kowol, J., Mancier, C., Sladkovic, R., Smit, H. G. J., Speth, P., Trickl, T. and Van Haver, P. 1997b. Task Group 3b: stratosphere–troposphere exchange — regional and global tropopause folding occurrence. In: *Transport and chemical transformation of pollutants in the troposphere, Final Report of the EUROTRAC Project, vol. 6, Tropospheric ozone research* (ed. Ø. Hov). Springer, Berlin, Germany, 131–151.

Bethan, S., Vaughan, G., Gerbig, C., Volz-Thomas, A., Richter, H. and Tiddeman, D. A. 1998. *J. Geophys. Res.* **103**, 13,413–13,434.

Bösenberg, J., Grabbe, G., Matthias, V. and Schaberl, T. 1997. Distribution and vertical transport of ozone in the lower troposphere determined by LIDAR. In: *Transport and chemical transformation of pollutants in the troposphere, Final Report of the EUROTRAC Project, vol. 6, Tropospheric ozone research* (ed. Ø. Hov). Springer, Berlin, Germany, 389–395.

Bristow, M. P., Bundy, D. H. and Wright, A. G. 1995. Signal linearity, gain stability, and gating in photomultipliers: application to differential absorption lidars. *Appl. Opt.* **34**, 4437–4452.

Broder, B., Dütsch, H. U. and Graber, W. 1981. Ozone fluxes in the nocturnal planetary boundary layer over hilly terrain. *Atmos. Environ.* **15**, 1195–1199.

Broder, B. and Gyax, H. A. 1985. The influence of locally induced wind systems on the effectiveness of nocturnal dry deposition of ozone. *Atmos. Environ.* **19**, 1627–1637.

Browell, E. V., Danielsen, E. F., Ismail, S., Gregory, G. L. and Beck, S. M. 1987. Tropopause fold structure determined from airborne lidar and in situ measurements. *J. Geophys. Res.* **92**, 2112–2120.

Carnuth, W. and Trickl, T. 2000. Transport studies with the IFU three-wavelength aerosol lidar during the

VOTALP Mesolcina experiment. *Atmos. Environ.* **34**, 1425–1434.

Claude, H. 1995, Monthly mean values for the height intervals 2.5 to 3.5 km, 3.5 to 4.5 km, and 6.5 to 7.5 km, kindly provided for the final report of TOR Task Group 1 (Scheel et al., 1997).

Drummond, J. W., Ehhalt, D. H. and Volz, A. 1988. Measurements of nitric oxide between 0–12 km altitude and 67 to 60°N latitude obtained during STRATOZ III. *J. Geophys. Res.* **93**, 15,831–15,849.

Eisele, H. 1997. *Aufbau und Betrieb eines Dreiwellenlängen-Lidars für Ozonmessungen in der gesamten Troposphäre und Entwicklung eines neuen Auswerteverfahrens zur Aerosolkorrektur*. Dissertation, Eberhard-Karls-Universität Tübingen, Germany, 107 pp (in German).

Eisele, H. and Trickl, T. 1997. Second Generation of the IFU stationary tropospheric ozone lidar. In: *Advances in atmospheric remote sensing with lidar* (eds. A. Ansmann, R. Neuber, P. Rairoux and U. Wandinger). Springer, Berlin, Germany, 379–382.

Eisele, H. and Trickl, T. 1998. Lidar sounding of tropospheric ozone at Garmisch-Partenkirchen. In: *Atmospheric ozone*, Proc. 1996 Quadrennial Ozone Symposium, vol. 1 (eds. R. D. Bojkov and G. Visconti). International Ozone Commission (Genève, Switzerland), 351–354.

Eisele, H., Scheel, H. E., Sladkovic, R. and Trickl, T. 1999. High-resolution lidar measurements of stratosphere–troposphere exchange, *J. Atmos. Sci.* **56**, 319–330.

Fehsenfeld, F. C. 1994. Transport of O_3 and O_3 precursors from anthropogenic sources to the North Atlantic. In: *Proceedings of EUROTRAC Symposium 1994* (eds. P. M. Borrell, P. Borrell, T. Cvitas and W. Seiler). SPB Academic Publishing, Den Haag, The Netherlands, 57–64.

Fehsenfeld, F. C., Daum, P., Leach, W. R., Trainer, M., Parrish, D. D. and Hübler, G. 1996. Transport and processing of O_3 and O_3 precursors over the North Atlantic: an overview of the 1993 North Atlantic Regional Experiment (NARE) summer intensive. *J. Geophys. Res.* **101**, 28,877–28,891.

Fishman, J., Vukovic, F. M. and Browell, E. V. 1985. The photochemistry of synoptic-scale ozone synthesis: implications for the global tropospheric ozone budget. *J. Atmos. Chem.* **3**, 299–320.

Furger, M., Dommen, J., Graber, W. K., Poggio, L., Prévôt, A., Emeis, S., Grell, G., Trickl, T., Gomiscek, B., Neininger, B. and Wotawa, G. 2000. The VOTALP Mesolcina Valley Campaign 1996 — concept, background and some highlights. *Atmos. Environ.* **34**, 1395–1412.

Harris, J. M. and Kahl, J. D. 1990. A descriptive atmospheric transport climatology for the Mauna Loa observatory, using clustered trajectories. *J. Geophys. Res.* **95**, 1909–1916.

Harris, J. M., Tans, P. P., Dlugokencky, E. J., Masarie, K. A., Lang, P. M., Whittlestone, S. and Steele, P. L. 1992. Variations in atmospheric methane at Mauna Loa observatory related to long-range transport. *J. Geophys. Res.* **97**, 6003–6010.

Höller, H., Finke, U., Huntrieser, H., Hagen, M. and Feigl, C. 1999. Lightning-produced NO_x (LINOX): experimental design and case study results. *J. Geophys. Res.* **104**, 13,911–13,922.

Iikura, Y., Sugimoto, N., Sasano, Y. and Shimzu, H. 1987. Improvement of lidar data processing for stratospheric aerosol measurements. *Appl. Opt.* **26**, 5299–5306.

Jacob, D. J., Logan, J. A., Gardner, G. M., Yevich, R. M., Spivakovsky, C. M., Wofsy, S. C., Sillman, S. and Prather, M. J. 1993. Factors regulating ozone over the United States and its export to the global atmosphere. *J. Geophys. Res.* **98**, 14,817–14,826.

Jäger, H., Carnuth, W. and Georgii, B. 1988. Observations of Saharan dust at a North Alpine mountain station. *J. Aerosol Sci.* **19**, 1235–1238.

Jäger, H. 1992. The Pinatubo eruption cloud observed by lidar at Garmisch-Partenkirchen. *Geophys. Res. Lett.* **19**, 191–194.

Kaiser, A. 1999. Die Bedeutung von Schadstoffmessungen im Hochgebirge am Beispiel des Sonnblick-Observatoriums — the importance of air chemistry measurements at high mountain sites taking the Sonnblick as an example. In: *Umweltforschung im Hochgebirge–Ergebnisse von GAW-DACH und verwandten Projekten*, Östereichische Beiträge zu Meteorologie und Geophysik, Heft 21. Zentralanstalt für Meteorologie und Geophysik (Wien, Austria), 5–13 (main text in German).

Kelly, N. A., Wolff, G. T. and Ferman, M. A. 1984. Sources and sinks of ozone in rural areas. *Atmos. Environ.* **18**, 1251–1266.

Kempfer, U., Carnuth, W., Lotz, R. and Trickl, T. 1994. A wide-range ultraviolet lidar system for tropospheric ozone measurements. *Rev. Sci. Instrum.* **65**, 3145–3164.

Kley, D., Crutzen, P. J., Smit, H. G. J., Vömel, H., Oltmans, S. J., Grassl, H. and Ramanathan, V. 1996. Observations of near-zero ozone concentrations over the convective Pacific: effects of air chemistry. *Science* **274**, 230–233.

Köhler, U. 1995. *Homogenization and re-evaluation of the long-term ozone series at the meteorological observatory Hohenpeissenberg*, Final Report of the DWD Project K/U 31. Deutscher Wetterdienst, Abteilung Forschung, Arbeitsergebnisse 31, Offenbach, Germany, 62 pp.

Langford, A. O., Masters, C. D., Proffitt, M. H., Hsie, E.-Y. and Tuck, A. F. 1996. Ozone measurements in a tropopause fold associated with a cut-off low system. *Geophys. Res. Lett.* **23**, 2501–2504.

Lee, H. S., Schwemmer, G. K., Korb, C. L., Dombrowski, M. and Prasad, C. 1990. Gated photomultiplier response characterization for DIAL measurements. *Appl. Opt.* **29**, 3303–3315.

Lin, X., Trainer, M. and Liu, S. C. 1998. On the nonlin-

earity of the tropospheric ozone production. *J. Geophys. Res.* **93**, 15,879–15,888.

Liu, S. C., McFarland, M., Kley, D., Zafiriou, O. and Huebert, B. 1983. Tropospheric NO_x and O_3 budgets in the equatorial Pacific. *J. Geophys. Res.* **88**, 1360–1368.

Liu, S. C., Trainer, M., Fehsenfeld, F. C., Parrish, D. D., Williams, E. J., Fahey, D. W., Hübler, G. and Murphy, P. C. 1987. Ozone production in the rural troposphere and the implications for regional and global ozone distributions. *Geophys. Res.* **92**, 4191–4207.

Logan, J. A. 1985. Tropospheric ozone: seasonal behavior, trends, and anthropogenic influence. *J. Geophys. Res.* **90**, 10,463–10,482.

Lugauer, M., Baltensberger, U., Furger, M., Gäggeler, H. W., Jost, D. T., Schwikowski, M. and Wanner, H. 1998. Aerosol transport to the high Alpine sites Jungfraujoch (3454 m asl) and Colle Gnifetti (4452 m asl). *Tellus* **50B**, 76–92.

McDermid, I. S., Godin, S. M. and Walsh, T. D. 1990. Lidar measurements of stratospheric ozone and intercomparisons and validation, *Appl. Opt*. **29**, 4914–4923.

MOH 1992. *Sonderbeobachtungen des Meteorologischen Observatoriums Hohenpeißenberg, Nr. 66, Ergebnisse der aerologischen und bodennahen Ozonmessungen.* ISSN 0581-1287 (ISSN 0343-7426), Hohenpeißenberg, Germany, 165 pp (in German).

Müller H. and Reiter, R. 1986. Untersuchung der Gebirgsgrenzschicht über einem großen Alpental bei Berg-Talwindzirkulation. *Meteorol. Rdsch.* **39**, 247–256 (in German).

Parrish, D. D., Holloway, J. S., Trainer, M., Murphy, P. C., Forbes, G. L. and Fehsenfeld, F. C. 1993. Export of North American ozone pollution to the North Atlantic ocean. *Science* **259**, 1436–1439.

Penkett, S. A., Reeves, C. E., Bandy, B. J., Kent, J. M. and Richter H. R. 1998. Comparison of calculated and measured peroxide data collected in marine air to investigate prominent features of the annual cycle of ozone in the troposphere. *J. Geophys. Res.* **103**, 13,377–13,388.

Pickering, K. E., Thompson, A. M., Dickerson, R. R., Luke, W. T., McNamara, D. P., Greenberg, J. P. and Zimmerman, P. R. 1990. Model calculations of tropospheric ozone production potential following observed convective events, *J. Geophys. Res.* **95**, 14,049–14,062; and references therein.

Proffit, M. H. and Langford, A. O. 1997. Ground-based differential absorption lidar system for day or night measurements of ozone throughout the free troposphere. *Appl. Opt*. **36**, 2568–2585.

Reichardt, J., Ansmann, A., Serwazi, M., Weitkamp, C. and Michaelis, W. 1996. Unexpectedly low ozone concentrations in midlatitude tropospheric ice clouds: a case study. *Geophys. Res. Lett*. **23**, 1929–1932.

Reiter, R., Müller, H., Sladkovic, R. and Munzert, K. 1983. Aerologische Untersuchungen der tagesperiodischen Gebirgswinde unter besonderer Berücksichtigung des Windfeldes im Talquerschnitt. *Meteorol. Rdsch.* **36**, 225–242 (in German).

Reiter, R., Müller, H., Sladkovic, R. and Munzert, K. 1984. Aerologische Untersuchungen des tagesperiodischen Windsystems im Inntal während MERKUR. *Meteorol. Rdsch.* **37**, 176–190 (in German).

Reiter, R., Kanter, H.-J. Munzert, K. and Sladkovic, R. 1985. *Wissenschaftliche Mitteilung Nr. 15*, Fraunhofer-Institut für Atmosphärische Umweltforschung. Garmisch-Partenkirchen, Germany (in German).

Reiter, R., Sladkovic, R. and Kanter, H.-J. 1987. Concentration of trace gases in the lower troposphere, simultaneously recorded at neighboring mountain stations, Part II. Ozone. *Meteorol. Atmos. Phys.* **37**, 27–47.

Reiter, R. 1990. The ozone trend in the layer of 2 to 3 km a.s.l. Since 1978 and the typical time variations of the ozone profile between ground and 3 km a.s.l. *Meteorol. Atmos. Phys.* **42**, 91–104.

Rudolph, J. 1988. Two-dimensional distribution of light hydrocarbons: results From the STRATOZ III experiment. *J. Geophys. Res.* **93**, 8367–8377.

Rudolph, J. 1995. The tropospheric distribution and budget of ethane. *J. Geophys. Res.* **100**, 11,369–11,381.

Scheel, H. E., Sladkovic, R. and Seiler, W. 1993. Ground-based measurements of ozone and related precursors at 47°N, 11°E. In: *EUROTRAC Annual Report 1992, Part 9, TOR*. EUROTRAC International Scientific Secretariat, Garmisch-Partenkirchen, Germany, 129–134.

Scheel, H. E., Ancellet, G., Areskoug, H., Beck, J., Bösenberg, J., De Muer, D., Dutot, A. L., Egelov, A. H., Esser, P., Étienne, A., Ferenczi, Z., Geiß, H., Grabbe, G., Granby, K., Gomiscek, B., Haszpra, L., Kezele, N., Klasinc, L., Laurila, T., Lindskog, A., Mowrer, J., Nielsen, T., Perros, P., Roemer, M., Schmitt, R., Simmonds, P., Sladkovic, R., Smit, H., Solberg, S., Toupance, G., Varotsos, C. and de Waal, L. 1997a. Spatial and Temporal Variability of Tropospheric Ozone over Europe. Final Report of TOR Task Group 1. In: *Transport and chemical transformation of pollutants in the troposphere, Final Report of the EUROTRAC Project, vol. 6, Tropospheric ozone research* (ed. Ø. Hov). Springer, Berlin, Germany, 35–64.

Scheel, H. E., Areskoug, H., Geiß, H., Gomiscek, B., Granby, K., Haszpra, L., Klasinc, L., Kley, D., Laurila, T., Lindskog, A., Roemer, M., Schmitt, R., Simmonds, P., Solberg, S., Toupance and G. 1997b. On the spatial distribution and seasonal variation of lower-troposphere ozone over Europe. *J. Atmos. Chem.* **28**, 11–28.

Scheel, H. E., Sladkovic, R. and Kanter, H.-J. 1999. Ozone variations at the Zugspitze (2962 m a.s.l.) during 1996–1997. In: *Proceedings of EUROTRAC Symposium 1998, vol. 1* (eds. P. M. Borrell and P. Borrell). WITPRESS, Southampton, Great Britain, 264–268.

Schwarz, R. and Steinbrecht, W. 1996. *Bestimmung der Förderleistung von Brewer-Mast-Ozonsondenpumpen in*

Abhängigkeit vom Luftdruck. Deutscher Wetterdienst, Abteilung Forschung und Entwicklung, Arbeitsergebnisse Nr. 35. Deutscher Wetterdienst, Offenbach, Germany, 33 pp (in German).

Seibert, P., Feldmann, H., Neininger, B., Bäumle, M. and Trickl, T. 2000. South Foehn and ozone in the Eastern Alps — case study and climatological aspects. *Atmos. Environ.* **34**, 1379–1394.

Singh, H. B., Viezee, W. and Salas, L. J. 1988. Measurements of selected C_2–C_5 hydrocarbons in the troposphere: latitudinal, vertical, and temporal variations. *J. Geophys. Res.* **93**, 15,861–15,878.

Singh, U. N., Ismail, S. and Schwemmer, G. K. (eds.) 1998. *Nineteenth International Laser Radar Conference*, Sessions on 'Tropospheric Profiling'. NASA Langley Center, Hampton, Virginia, USA, 257–311 and 367–476.

Sladkovic, R., Scheel, H. E. and Seiler, W. 1994. Ozone climatology at the mountain sites, Wank and Zugspitze. In: *Proceedings of EUROTRAC Symposium 1994* (eds. P. M. Borrell, P. Borrell, T. Cvitas and W. Seiler). SPB Academic Publishing, Den Haag, The Netherlands, 253–258.

Sladkovic, R., Scheel, H. E. and Seiler, W. 1997. Interpretation of ozone concentrations at three alpine sites based on statistical and trajectory analyses. In: *Proceedings of EUROTRAC Symposium 1996* (eds. P. M. Borrell, P. Borrell, K. Kelly, T. Cvitas and W. Seiler). Computational Mechanics Publications, Southampton, Great Britain, 943–947.

Steinbrecht, W., Schwarz, R. and Claude, H. 1998. New pump correction for the Brewer-Mast ozone sonde: determination from experiment and instrument intercomparisons. *J. Atmos. Oceanic Technol.* **15**, 144–156.

Stockwell, W. R., Junkermann, W., Walcek, C. J. and Yuan, H.-H. 1996. The influence of clouds on the photochemistry of tropospheric ozone: the effect of cloud water scavenging on HO_2 radical concentrations. In: *Proc. 89th Annual Meeting of the Air & Waste Management Association*, Nashville, Tennessee, 23–28 June 1996, paper 96-FA130B.01, 9 pp.

Stohl, A. and Trickl, T. 1999. A textbook example of long-range transport: simultaneous observation of ozone maxima of stratospheric and North American origin in the free troposphere over Europe. *J. Geophys. Res.* **104**, 30,445–30,462.

Stohl, A. and Trickl, T. 2000. Observation of high ozone concentrations over central Europe during episodes of intercontinental transport. In: *Atmospheric ozone, Proceedings of the Quadrennial Ozone Symposium 2000*, Sapporo, Japan, 10–14 July 2000. NASDA, Tokyo, Japan, 653–654.

TESLAS 1997. Tropospheric environmental studies by laser sounding (TESLAS). In: *Transport and chemical transformation of pollutants in the troposphere, Final Report of the EUROTRAC Project, vol. 8, Instrument development for atmospheric research and monitoring* (eds. J. Bösenberg, D. Brassington and P. C. Simon). Springer, Berlin, Germany, 1–203.

TOR 1997. *Transport and chemical transformation of pollutants in the troposphere, Final Report of the EUROTRAC Project, vol. 6, Tropospheric ozone research* (ed. Ø. Hov). Springer, Berlin, Germany, 499 pp.

TOR 1997a. *J. Atmos. Chem.* **28**, 1–359.

Vergeiner, I. and Dreiseitl, E. 1987. Valley winds and slope winds — observations and elementary thoughts. *Meteorol. Atmos. Phys.* **36**, 264–286.

Volz, A. and Kley, D. 1988. Evaluation of the Montsouris series of ozone measurements made in the nineteenth century. *Nature* **332**, 240–242.

Volz, A., Geiss, H., McKeen, S. and Kley, D. 1989. Correlation of ozone and solar radiation at Montsouris and Hohenpeißenberg: indications for photochemical influence. In: *Ozone in the atmosphere* (eds. R. D. Bojkov and P. Fabian). A. Deepak Publishing, Hampton, Virginia, USA, 447–450.

VOTALP 2000. *Atmos. Environ.* **34**, 1319–1453.

Weller, R., Lilischkis, R., Schrems, O., Neuber, R. and Wessel, S. 1996. Vertical ozone distribution in the marine atmosphere over the Atlantic Ocean (56°S–50°N). *J. Geophys. Res.* **101**, 1387–1399.

Wild, O., Law, K. S., McKenna, D. S., Bandy, B. J., Penkett, S. A. and Pyle, J. A. 1996. Photochemical trajectory modeling studies of the North Atlanic region during August 1993. *J. Geophys. Res.* **101**, 29,269–29,288.